



Clay exfoliation and polymer/clay aerogels by supercritical carbon dioxide

Simona Longo¹, Marco Mauro¹, Christophe Daniel¹, Maurizio Galimberti^{2,3} and Gaetano Guerra^{1*}

¹ Department of Chemistry and Biology and INSTM Research Units, Università degli Studi di Salerno, Fisciano, Italy

² Department of Chemistry, Materials and Chemical Engineering, Politecnico di Milano, Milano, Italy

³ CNR, Istituto per lo Studio delle Macromolecole, National Research Council, Milano, Italy

Edited by:

Giuseppe Mensitieri, University of Naples Federico II, Italy

Reviewed by:

Giuseppe Mensitieri, University of Naples Federico II, Italy

Ernesto Di Maio, University of

Naples Federico II, Italy

Giovanni Filippone, University of

Naples Federico II, Italy

*Correspondence:

Gaetano Guerra, Department of Chemistry and Biology and INSTM Research Units, Università degli Studi di Salerno, Via Giovanni Paolo II 132, 84084 Fisciano, Italy
e-mail: gguerra@unisa.it

Supercritical carbon dioxide (scCO₂) treatments of a montmorillonite (MMT) intercalated with ammonium cations bearing two long hydrocarbon tails (organo-modified MMT, OMMT) led to OMMT exfoliation, with loss of the long-range order in the packing of the hydrocarbon tails and maintenance of the long-range order in the clay layers. The intercalated and the derived exfoliated OMMT have been deeply characterized, mainly by X-ray diffraction analyses. Monolithic composite aerogels, with large amounts of both intercalated and exfoliated OMMT and including the nanoporous-crystalline δ form of syndiotactic polystyrene (s-PS), have been prepared, by scCO₂ extractions of s-PS-based gels. Also for high OMMT content, the gel and aerogel preparation procedures occur without re-aggregation of the exfoliated clay, which is instead observed for other kinds of polymer processing. Aerogels with the exfoliated OMMT have more even dispersion of the clay layers, higher elastic modulus and larger surface area than aerogels with the intercalated OMMT. Extremely light materials with relevant transport properties could be prepared. Moreover, s-PS-based aerogels with exfoliated OMMT could be helpful for the handling of exfoliated clay minerals.

Keywords: cationic clays, organoclays, montmorillonite, syndiotactic polystyrene, nanoporous-crystalline δ form, monolithic aerogels

INTRODUCTION

Over the last decades, clay polymer nanocomposites (CPN) (LeBaron et al., 1999; Alexandre and Dubois, 2000; Ray and Okamoto, 2003; Bergaya, 2008; Chen et al., 2008; Galimberti, 2011) have been steadily increasing their importance in the field of material science, as they substantially improve polymer properties such as mechanical reinforcement, impermeability, thermal stability (Paul and Robeson, 2008; Bergaya and Lagaly, 2013). Superior properties are achieved when individual clay layers or stacks of few layers are evenly distributed in the polymer matrix and polymer-clay interfaces are maximized (Kojima et al., 1993; Vaia et al., 1993; Manias et al., 2001).

CPN exhibiting exfoliated clays are difficult to attain, particularly in the case of non-polar polymers (Choi et al., 2004; Robello et al., 2004; Chou and Lin, 2005; Galimberti et al., 2007, 2009, 2010).

Many reports show that different processing techniques based on supercritical carbon dioxide (scCO₂) constitute effective ways to increase dispersion and delamination in polymer/clay nanocomposites (Ma et al., 2007; Nguyen and Baird, 2007; Treece and Oberhauser, 2007; Samaniuk et al., 2009; Baker et al., 2011; Feng-hua et al., 2011; Chen et al., 2012). However, X-ray characterization of most samples show the presence of basal 00l reflections, clearly indicating that treatments with scCO₂ are generally unsui to induce complete organoclay exfoliation (Ma et al., 2007; Nguyen and Baird, 2007; Treece and Oberhauser, 2007; Samaniuk et al., 2009; Thompson et al., 2009; Baker et al., 2011; Feng-hua et al., 2011; Chen et al., 2012).

Only some reports, from the Kannan's group, show that a complete disappearance of the 00l reflections (and hence a complete exfoliation) can be achieved by scCO₂ treatments on pure organoclays, where alkali counterions have been exchanged with long-chain alkylammoniums (Horsch et al., 2006; Manitiu et al., 2008). However, as a consequence of preparation of polymer nanocomposites, the 00l reflections reappear with peak height and location essentially independent of the processing conditions (Manitiu et al., 2008).

scCO₂ treatments are also effective to prepare monolithic aerogels, by drying of wet gels. Aerogels constitute a unique class of materials, characterized by a highly porous network being attractive for many applications such as thermal and acoustic insulation, capacitors or catalysis (Kistler, 1931; Schaefer and Keefer, 1986; Anderson et al., 2002; Malik et al., 2006; Wei et al., 2010; Kucheyev et al., 2012; Longo et al., 2013). In recent years, the scCO₂ extraction of gels of suitable thermoplastic polymers, like syndiotactic polystyrene (s-PS) (De Rosa et al., 1997; Milano et al., 2001; Gowd et al., 2006; Rizzo et al., 2007; Petraccone et al., 2008) and poly(2,6-dimethyl-1,4-phenylene)oxide, (Daniel et al., 2011, 2013a,b; Galizia et al., 2012; Tarallo et al., 2012) has allowed the preparation of a special class of monolithic aerogels, (Daniel et al., 2005, 2008, 2009, 2012, 2013a,b; Wang and Jana, 2013) that present, beside disordered amorphous micropores (typical of all aerogels), identical nanopores of *nanoporous-crystalline* phases. Many studies show that nanoporous-crystalline polymer phases are able to absorb low molecular-mass molecules also when present in traces and are suitable for molecular separation

(Manfredi et al., 1997; Musto et al., 2002; Mahesh et al., 2005; Venditto et al., 2006; Albulnia et al., 2013), sensor (Mensitieri et al., 2003; Giordano et al., 2005; Cusano et al., 2006; Buono et al., 2009; Pilla et al., 2009; Erdogan et al., 2012) and catalysis (Buonerba et al., 2012) applications.

A first aim of the present paper is a deeper investigation of the scCO₂ induced organoclay exfoliation, by a more complete X-ray diffraction characterization of organoclays before and after scCO₂ treatments. The second aim of the paper is the preparation of composite aerogels containing large amounts of exfoliated organoclay as well as a nanoporous-crystalline polymer phase. The basic idea is that aerogel preparation processes, also based on scCO₂ extraction, could help to maintain the clay exfoliation, which is generally lost in the nanocomposite processing (Manitiu et al., 2008). Advanced properties are pursued, through the synergy of aerogels and exfoliated clays. A montmorillonite (MMT) intercalated with dimethyl di(hydrogenated tallow) (2HT) ammonium cation was selected as the organoclay (OMMT in the following).

MATERIALS AND METHODS

MATERIALS

Organically modified MMT, trade name Dellite® 67G, with 40 wt % of di(hydrogenated tallow)-dimethylammonium (2HT) was purchased from Laviosa Chimica Mineraria S.p.A.

The sPS used in this study was manufactured by Dow Chemicals under the trademark Questa 101. ¹³C nuclear magnetic resonance characterization showed that the content of syndiotactic triads (Grassi et al., 1987) was over 98%. The mass average molar mass obtained by gel permeation chromatography (GPC) in trichlorobenzene at 135°C was found to be $M_w = 3.2 \times 10^5$ g mol⁻¹ with a polydispersity index $M_w/M_n = 3.9$.

1,2-dichlorobenzene (DCB), used for clay dispersions, was purchased from Aldrich and used without further purification.

CLAY DELAMINATION AND EXFOLIATION BY scCO₂

Exfoliated clay samples were obtained by using a SFX 200 supercritical carbon dioxide extractor (ISCO Inc.). Organically modified clays (typically 10 mg in a 20 mL stainless steel vessel) were processed in scCO₂ at 40°C and 200 bar, for 16 and 32 h under quiescent conditions, in order to promote the diffusion of the supercritical fluid into the clay interlayer space. The system was then rapidly depressurized (1 min) to atmospheric pressure and the expansion of the scCO₂ between the layers caused the clay exfoliation.

PREPARATION OF sPS/CLAY GELS

Dispersions of the clays in DCB were obtained with both as received and exfoliated samples. A clay dispersion was initially prepared by adding the appropriate clay amount in 5 ml of DCB. The mixtures were homogenized for 1 h under magnetic stirring and sonicated in a 5000 mL batch bath ultrasound (Badelin Sonorex RK 1028 H) for 1 h.

sPS/clay gels were prepared, in hermetically sealed test tubes, by heating the clay dispersions above the boiling point of the solvent until complete dissolution of the polymer and the appearance of a transparent and homogeneous solution had occurred.

The hot solution was then cooled to room temperature, where gelation occurred. For instance, 655 mg of sPS and 5 mL of 2 wt % clay dispersion were mixed to obtain clay/polymer gels. The overall amount of polymer and clay in the gels was generally fixed to 10 wt %.

PREPARATION OF sPS/CLAY AEROGELS

Aerogels were obtained by treating sPS/clay gels with a SFX 200 supercritical carbon dioxide extractor (ISCO Inc.) using the following conditions: $T = 40^\circ\text{C}$, $P = 200$ bar, extraction time $t = 6$ h. The prepared s-PS/clay aerogels present a weight composition ranging between 96/4 and 50/50. The aerogels, as prepared from gels with an overall polymer-clay content of 10 wt %, present a porosity close to 90%.

For monolithic aerogels with a regular cylindrical shape, the total porosity can be estimated from the mass/volume ratio of the aerogel. Then, the percentage of porosity P of the aerogel samples can be expressed as:

$$P = 100 * [1 - (\rho_{\text{app}}/\rho_{\text{pol}})] \quad (1)$$

where ρ_{pol} is the density of the polymer matrix and ρ_{app} is the aerogel apparent density calculated from the mass/volume ratio of the monolithic aerogels.

CHARACTERIZATION TECHNIQUES

Wide angle X-ray diffraction

Wide-angle X-ray diffraction (WAXD) patterns with nickel filtered Cu-K α radiation were obtained, with an automatic Bruker D8 Advance diffractometer, in reflection. The intensities of the WAXD patterns were not corrected for polarization and Lorentz factors, to allow an easier comparison with most literature data. The D_{hkl} correlation length of crystals was determined applying the Scherrer equation:

$$D_{\text{hkl}} = K\lambda/(\beta_{\text{hkl}}\cos\theta_{\text{hkl}}) \quad (2)$$

where: K is the Scherrer constant, λ is the wavelength of the irradiating beam (1.5419 Å, CuK α), β_{hkl} is the width at half height, and θ_{hkl} is the diffraction angle. The instrumental broadening, b , was determined by obtaining a WAXD pattern of a standard silicon powder 325 mesh (purity >99%), under the same experimental conditions. For each observed reflection with $\beta_{\text{hkl}} < 1^\circ$, the width at half height was evaluated by subtracting the unavoidable instrumental broadening of the closest silicon reflection from the experimental width at half height, β_{hkl} , using the following relationship:

$$\beta_{\text{hkl}}^2 = (B_{\text{hkl}}^2 - b^2) \quad (3)$$

Scanning electron microscopy

The internal morphology of the aerogels was characterized by means of a scanning electron microscope (SEM, Zeiss Evo50 equipped with an Oxford energy dispersive X-ray detector). Samples were prepared by fracturing small pieces of the monoliths in order to gain access to the internal part of the specimen. In fact, the external lateral surfaces of most samples were found to

be flat and free of porosity. Low energy was used (5 keV) to obtain the highest possible surface resolution. Before imaging, all specimens were coated with gold using a VCR high resolution indirect ion-beam sputtering system. The samples were coated depositing approximately 20 nm of gold. The coating procedure was necessary to prevent surface charging during measurement and to increase the image resolution.

BET measurements

Nitrogen adsorption at liquid nitrogen temperature (77 K) was used to measure surface areas of OMMT and polymer/OMMT aerogels with a Nova Quantachrome 4200e instrument. Before the adsorption measurement, OMMT powders were degassed at 100°C under vacuum for 24 h, while polymer/clay aerogels were degassed at 40°C, in the same conditions. The surface area values were determined by using 11-point BET analysis.

Differential scanning calorimetry

The differential scanning calorimetry (DSC) of OMMT powders and polymer/OMMT aerogels was carried out under nitrogen from 0 to 300°C at a heating rate of 10°C/min on a TA instruments DSC 2920.

Dynamic-mechanical analysis

Dynamic-mechanical properties were studied using a Triton dynamic-mechanical thermal analyzer. The spectra were recorded in the three-point bending mode, on samples with the following dimensions: length 15 mm, width 10 mm, and thickness 2 mm. The modulus E' was obtained, as a function of temperature, at a frequency of 1 Hz and an amplitude of 0.03 mm. The heating rate was 2°C/min in the range of 0, +100°C.

RESULTS AND DISCUSSION

OMMT EXFOLIATION BY scCO_2

The X-ray diffraction ($\text{CuK}\alpha$) pattern in the 2θ range 2–80° of the OMMT, with 40 wt % of 2HT, is reported in **Figure 1A**. Besides many $00l$ reflections (up to $l = 12$) that indicate a high degree of order perpendicular to the clay layers and an interlayer spacing of 3.5 nm, the pattern shows well defined weak peaks, corresponding to the typical 020, 210, and 060 in-plane MMT periodicities (Galimberti et al., 2007; Powder diffraction database 70-2151 International Centre for Diffraction Data, 1999). It is worth adding that a well defined narrow peak is also present at $2\theta = 21.7^\circ$, corresponding to $d = 0.41$ nm, i.e., the distance between long hydrocarbon chains in their rotator order, analogous to those observed for long-chain alkylammoniums intercalated in anionic clays (layered double hydroxide, LDH) (Itoh et al., 2003) as well as in graphite oxide (Mauro et al., 2013). The thickness of the clay layer (≈ 1 nm) and the length of the alkylammoniums (≈ 5 nm) (Osman et al., 2002) indicate that the tilting angle of the hydrocarbon chains is not far from $\alpha = 60^\circ$. Hence, the X-ray diffraction pattern of **Figure 1A** indicates the presence of a MMT/2HT intercalate structure, whose schematic projections, parallel and perpendicular to the clay layers, are shown in **Figures 2A,B**, respectively.

The X-ray diffraction patterns of the OMMT of **Figure 1A**, after short term and long term treatments by scCO_2 are shown in **Figures 1B,C**, respectively. For the intermediate pattern of **Figure 1B**, the intensities of the $00l$ peaks as well as of the rotator order peak (100r) are strongly reduced (see also the inset of **Figure 1B**). The in-plane 020, 210, and 060 peaks maintain their intensity and narrowness. This indicates that short term

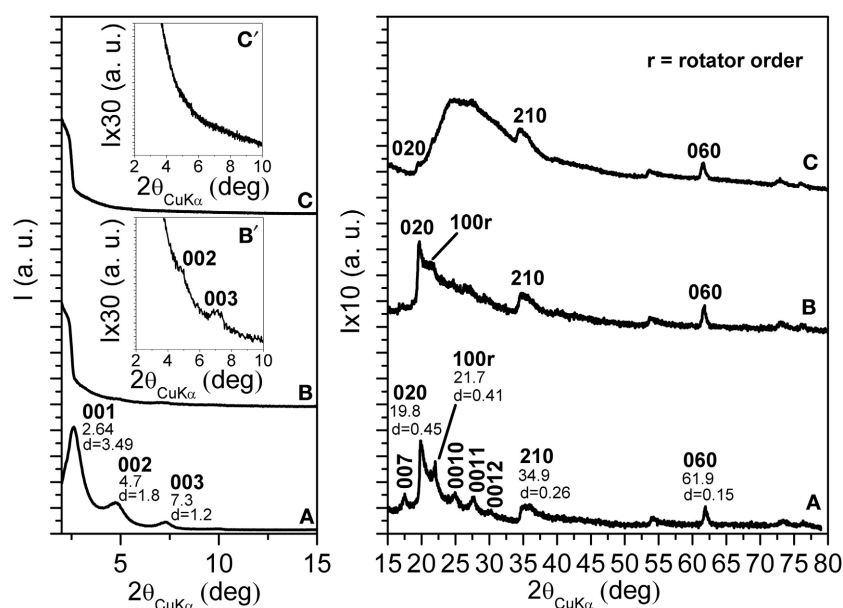
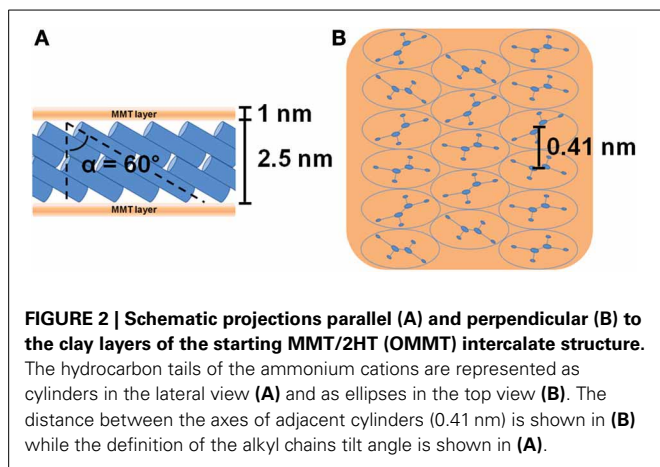


FIGURE 1 | X-ray diffraction ($\text{CuK}\alpha$) patterns in the 2θ range 2–80° of MMT, as intercalated with 40 wt % of 2HT ammonium before (A) and after 16 h (B) and 32 h (C) scCO_2 treatments. The inset in (B) and (C)

enlarges the 2θ range 2–10°. The Miller index 100r indicate the reflection relative to the rotator order of the long hydrocarbon chains within the interlayer space.



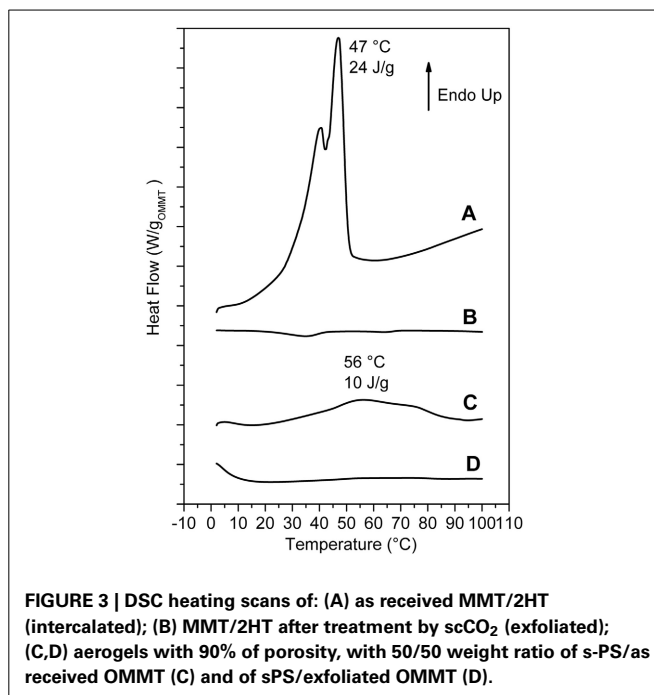
scCO₂ treatments lead to a nearly complete clay exfoliation with maintenance of the in-plane order.

In agreement with previous results (Manitiu et al., 2008), the X-ray diffraction pattern of the OMMT, after long-term scCO₂ treatments, does not show anymore the 00*l* reflections (see also the inset of Figure 1C): clay exfoliation is achieved. It is worth adding that the in-plane 020, 210, and 060 reflections are still present, although become less intense than a broad amorphous halo that appears in the 2θ range 20–30°. This amorphous halo can be attributed to a loss of order in the stacking of the clay layers, also associated with a complete loss of order in the packing of the hydrocarbon tails.

In summary, the described long-term scCO₂ treatments lead to exfoliation of the OMMT, and to a complete loss of long-range lateral order of the hydrocarbon tails of the cationic surfactant. The maintenance of hk0 reflections (mainly of the isolated 060 reflection), not yet reported in the literature, assures the maintenance of a long-range order in the clay layers. In this respect, it is worth adding that the half-height width of the 060 reflection, after exfoliation, remains equal to 0.45° indicating a correlation length $D_{060} = 28$ nm.

Relevant additional information, relative to the as received and scCO₂-treated OMMT, can be obtained by DSC scans (Figure 3). The scan of the as received OMMT (Figure 3A) presents a reversible transition nearly located at 44°C ($\Delta H \approx 26$ J/g) that corresponds to the loss of rotator order of the hydrocarbon tails of the cations intercalated in the interlayer space. In this respect, it is worth adding that endothermic peaks corresponding to the loss of order in the packing of the hydrocarbon tails have been observed, in the temperature range 25–80°C, not only for cationic organoclays, (Cipolletti et al., 2013) but also for other organically modified layered inorganic structures (Ide and Ogawa, 2006) as well as for graphite oxide intercalation compounds (Mauro et al., 2013). The DSC scan of the scCO₂ treated OMMT does not present any thermal transition in the considered temperature range (Figure 3B) and hence indicates the loss of 3D order in the packing of the hydrocarbon tails of the ammonium surfactant, which is compatible with clay exfoliation.

The overall information arising from X-ray diffraction and DSC characterization allows to conclude that the as received



and scCO₂ treated OMMT can be described as intercalated and exfoliated OMMT, respectively.

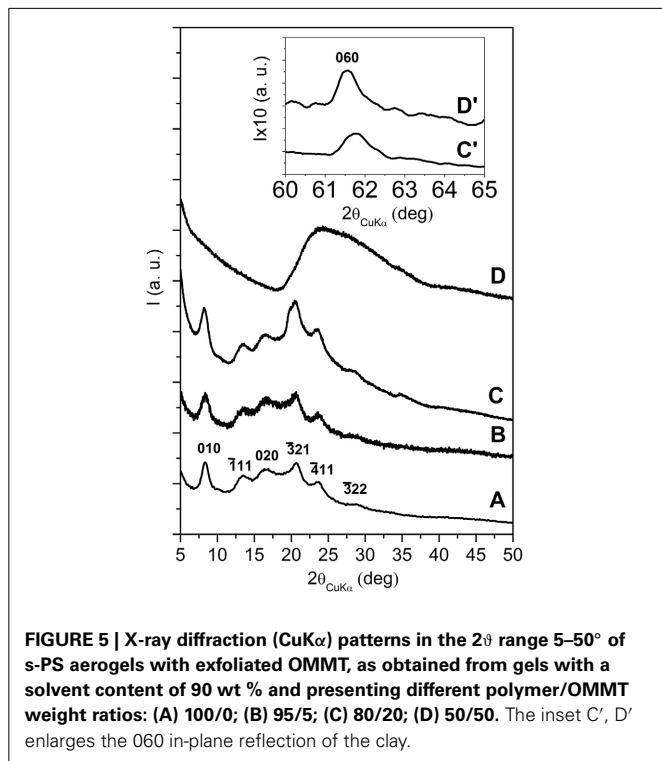
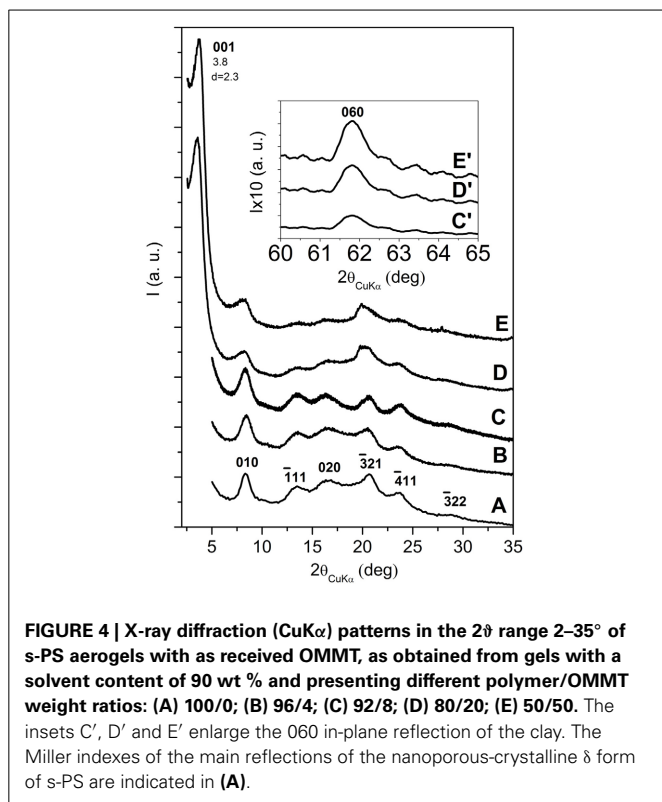
MONOLITHIC NANOPOROUS-CRYSTALLINE s-PS AEROGELS WITH LARGE OMMT CONTENT

Monolithic composite aerogels, filled with large fractions of intercalated and exfoliated OMMT, have been prepared by using an s-PS matrix. This polymer choice is mainly due to the ability of s-PS to produce monolithic aerogels in a very broad range of porosity (from 50% up to 99%). An additional reason for this choice is the easy obtainment of aerogels exhibiting s-PS nanoporous-crystalline δ (Daniel et al., 2005, 2008) or ϵ (Daniel et al., 2009) phases.

Aerogels with a porosity of nearly 90% were obtained by scCO₂ extraction of gels with a DCB content of 90 wt % and with different s-PS/OMMT weight ratios. For all aerogels with polymer/OMMT ratio equal or higher than 80/20, monolithic structures were obtained. Moreover, as usual for s-PS based aerogels, (Daniel et al., 2005, 2008, 2009, 2012, 2013a,b) the size and shape of s-PS/clay aerogels are essentially the same of the precursor gels. Aerogels with a 50/50 polymer/OMMT ratio are brittle and are generally obtained as powders.

X-ray diffraction (CuK α) patterns of s-PS based aerogels, containing intercalated and exfoliated OMMT, are shown in Figures 4, 5, respectively.

All patterns of Figure 4 show the typical reflections of the nanoporous-crystalline δ form. In particular, the isolated intense 010 reflection is always clearly apparent and located at $2\theta \approx 8.4^\circ$. The 00*l* reflections of the OMMT are not detected for the aerogels with low clay content (4 and 8 wt %) while for higher clay contents (20 and 50 wt %) a narrow and intense 001 reflection is present, while the 002 and 003 reflections of the starting clay have disappeared. Moreover, the



001 reflection is markedly shifted with respect to its original position (from $2\theta = 2.6^\circ$ up to $2\theta = 3.8^\circ$), indicating a decrease of the interlayer spacing from $d = 3.5$ nm down to $d = 2.3$ nm.

The results of **Figures 4A–C** suggest that the aerogel preparation procedure involving $scCO_2$ extraction, for low OMMT content, could lead to clay exfoliation, as already observed for $scCO_2$ treatment of the neat OMMT in **Figure 1**. **Figures 4C,D** show that, for high OMMT content in the aerogels, the used procedure is not suitable to generate OMMT exfoliation but, on the contrary, a reduction of the interlayer spacing is observed. An analogous phenomenon of reduction of interlayer spacing has been recently observed for organoclay extraction with different solvents, like e.g., ethyl acetate (Cipolletti et al., 2013). As suggested in that paper, the observed reduction of basal spacing can be attributed to the extraction of excess cationic surfactant, not being ionically bonded to the negatively charged clay layers, but being simply included in the interlayer space by non-bonded interactions and contributing to the crystalline order of the hydrocarbon tails.

Additional information on the structural organization in the s-PS/OMMT aerogels comes from DSC analyses. In particular, DSC heating scan of a 50/50 by wt. s-PS/as-received-clay aerogel is shown in **Figure 3C**. The endothermic peak, corresponding to loss of rotator order in the interlayer spacing (**Figure 1A**) becomes broader and its maximum is shifted up to 50–60°C, with only a minor reduction of the related enthalpy ($\Delta H_r \approx 10$ J/g ≈ 20 J/gOMMT).

The combined information of the X-ray diffraction patterns of **Figures 4C,D** and the DSC scans of **Figure 3C** indicates that, for high clay content, the aerogel preparation procedure brings to a reduction of the OMMT basal spacing (d_{001}) from 3.5 nm down to 2.3 nm, with only partial loss of the hydrocarbon rotator order in the interlayer space.

The X-ray diffraction patterns of the s-PS aerogels prepared with the exfoliated OMMT (**Figure 5**), independently of the aerogel composition, do not show 00 l clay reflections, while show the isolated weak 060 in-plane clay reflection (as shown by the inset of **Figures 5C',D'**). This clearly indicates that the gel and aerogel preparation procedures, also for high clay concentrations, allow to maintain clay exfoliation without re-aggregation, as instead observed for other common polymer processing (Nguyen and Baird, 2007; Manitiu et al., 2008).

In this respect, it is worth citing that X-ray diffraction patterns of polymer-clay aerogels as obtained by freeze-drying of polymer solutions including clays (Bandi et al., 2005; Pojanavaraphan et al., 2010, 2011; Wang et al., 2013) show the presence of 00 l clay reflections, (Pojanavaraphan et al., 2010; Wang et al., 2013), which exclude the occurrence of exfoliation.

The patterns of **Figure 5** also show that s-PS is generally crystallized in the nanoporous δ form (**Figures 5A–C**) while, for the 50/50 polymer/exfoliated-OMMT aerogel, the s-PS crystallization does not occur (broad amorphous halo of **Figure 5D**). This is probably due to the good dispersion of a large amount of exfoliated OMMT, leading to a diluting effect on sPS that reduces its crystallization kinetics. This loss of polymer crystallinity leads to a loss of the typical fibrillar structure, which in turn allows rationalizing the loss of monolithic structure.

COMPARISON BETWEEN AEROGELS WITH INTERCALATED AND EXFOLIATED OMMT

This section presents a strict comparison between properties of s-PS monolithic aerogels exhibiting a porosity of 90% and a OMMT content of 20 wt %, as obtained by using intercalated or exfoliated OMMT, that present the X-ray diffraction patterns shown in **Figures 4D, 5C**, respectively.

On the basis of quantitative evaluations on the X-ray diffraction patterns, the two aerogels present similar degree of polymer crystallinity ($\approx 40\%$). However, aerogels with the exfoliated clay (**Figure 6A**) are much more homogeneous than aerogels obtained with the intercalated OMMT (**Figure 6B**), which clearly present rough surfaces.

Also the SEM images of the two aerogels are completely different. In fact, the SEM of the aerogel including the intercalated OMMT is dominated by the micrometric OMMT particles (**Figure 7B**) while the SEM of the aerogel including the exfoliated OMMT (**Figure 7A**) clearly shows both nanometric clay platelets and nanometric s-PS fibrils (**Figure 7A'**).

The results of the SEM analyses suggest that also the large difference in the visual appearance between the two aerogels of **Figure 6** could be due to micrometric and nanometric size of intercalated and exfoliated clays, respectively.

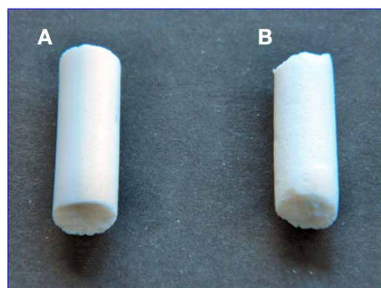


FIGURE 6 | Photographs of cylindrical monolithic (diameter of 7 mm) s-PS/OMMT aerogels, with porosity $P = 90\%$, as obtained by $scCO_2$ drying and exhibiting a 80/20 weight ratio: (A) with exfoliated clay; (B) with intercalated clay. The shown aerogels essentially present the same size and shape of the precursor gels.

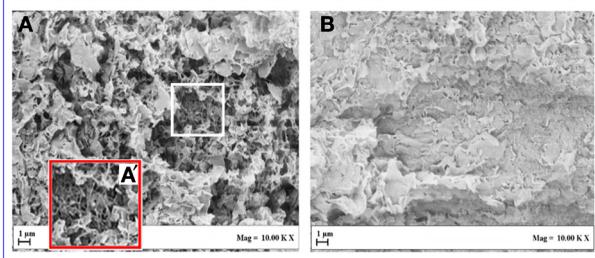


FIGURE 7 | SEM of aerogels with porosity $P = 90\%$, having 80/20 polymer/OMMT weight ratio: (A,A') with exfoliated OMMT; (B) with intercalated OMMT.

DMA analyses indicate that aerogels based on the exfoliated clay present an elastic modulus definitely higher than for those based on intercalated OMMT (36 MPa vs. 15 MPa).

Surface areas S_{BET} , as obtained by N_2 adsorption data at 77 K, for the intercalated and exfoliated OMMT, as well as those of the corresponding aerogels, are compared in **Table 1**. For the sake of comparison, S_{BET} of the neat s-PS aerogel presenting the same porosity is shown in the last row of **Table 1**. As well known, s-PS aerogels exhibit high surface areas, mainly associated with the crystalline cavities of the δ crystalline phase, but also associated with the amorphous aerogel porosity (Daniel et al., 2005, 2008, 2009, 2012, 2013a,b). In agreement with literature data, (Park et al., 2011) S_{BET} of the OMMT is rather low and is substantially increased for the exfoliated OMMT ($S_{BET} = 18 \text{ m}^2/\text{g}$). The s-PS/exfoliated-clay aerogels present values of S_{BET} ($281 \text{ m}^2\text{g}^{-1}$) much higher than those of the s-PS/intercalated-clay aerogels ($166 \text{ m}^2\text{g}^{-1}$) and not far from those observed for pure s-PS aerogels ($312 \text{ m}^2\text{g}^{-1}$). This indicates that, also for this high OMMT content (20 wt %), the exfoliated clay not only does not disturb the formation of the nanoporous crystalline phase but also does not alter the amorphous aerogel porosity.

A schematic representation of the sPS/exfoliated-OMMT aerogels is shown in **Figure 8**.

CONCLUSIONS

A thorough investigation of $scCO_2$ -induced exfoliation of OMMTs has been conducted mainly by X-ray diffraction and DSC characterization techniques. The starting material is a MMT intercalated with ammonium cations bearing two long hydrocarbon tails. Suitable $scCO_2$ treatments led to exfoliation of the

Table 1 | Total surface area (S_{BET}) of OMMT samples and of aerogels with porosity $P = 90\%$, having 80/20 polymer/OMMT weight ratio.

Sample	S_{BET}^a (m^2g^{-1})
Intercalated OMMT	10
Exfoliated OMMT ($scCO_2$ treated)	18
sPS/intercalated-OMMT, 80/20 aerogel	166
sPS/exfoliated-OMMT, 80/20 aerogel	281
Aerogel δ sPS	312

^aTotal area evaluated following the BET model in the standard $0.05 < P/P_0 < 0.3$ pressure range.

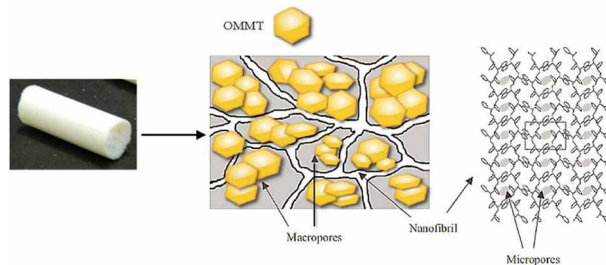


FIGURE 8 | Schematic representation of the sPS/exfoliated-OMMT aerogels.

OMMT and also led to a complete loss of long-range order in the packing of the hydrocarbon tails of the cationic surfactant. The maintenance of hk0 reflections (mainly of the isolated 060 reflection), not yet reported in the literature, assures the maintenance of a long-range order in the clay layers. DSC scans of the intercalated OMMT present a reversible transition that corresponds to the loss of rotator order of the hydrocarbon chains in the interlayer spacing while those of the exfoliated OMMT do not present any thermal transition up to 100°C. This confirms the absence of any 3-D order for the exfoliated clay.

Monolithic composite aerogels, filled with large amounts of both intercalated and exfoliated OMMT, have been prepared, starting from s-PS-based gels. In particular, for aerogels with high content of the intercalated OMMT, the preparation procedure brings to a reduction of the basal spacing (d_{001}) from 3.5 nm down to 2.3 nm, with only partial loss of the hydrocarbon rotator order in the interlayer space. For aerogels with high content of the exfoliated OMMT, the gel and aerogel preparation procedures allow to maintain clay exfoliation without re-aggregation, as instead observed for other common polymer processing.

A strict comparison between s-PS monolithic aerogels with a porosity of 90% and a OMMT content of 20 wt %, as obtained by using intercalated or exfoliated OMMT, has been also reported. Although the two aerogels present similar degree of polymer crystallinity ($\approx 40\%$) as well as the same polymer crystalline form (the nanoporous-crystalline δ form), aerogels with the exfoliated OMMT are much more homogeneous than aerogels with the intercalated OMMT. This difference, clearly apparent both on visual inspection as well as on SEM analysis, is due to micrometric and nanometric size of intercalated and exfoliated clays, respectively. Aerogels based on the exfoliated clay also present elastic modulus definitely higher than those based on intercalated OMMT. Moreover, s-PS/exfoliated-clay aerogels present values of surface area ($281 \text{ m}^2 \text{ g}^{-1}$) much higher than those of the s-PS/intercalated-clay aerogels ($166 \text{ m}^2 \text{ g}^{-1}$) and not far from those observed for pure s-PS aerogels ($312 \text{ m}^2 \text{ g}^{-1}$). This indicates that, also for high content, the exfoliated clay does not alter the aerogel porosity.

The improvement of properties such as the modulus and the surface area is definitely of interest in view of potential applications of aerogels with exfoliated OMMT, for example for achieving relevant transport properties with extremely light materials. Moreover, the clay rich aerogels (e.g., 50/50, w/w), could be helpful to an easier handling of exfoliated OMMT, removing the risks connected with inhalable nanoparticles.

ACKNOWLEDGMENTS

We thank Dr. Luca Giannini, Dr. Angela Lostritto and Dr. Valeria Cipolletti of Pirelli Tyre Research Center, for useful discussions. Financial support of “Ministero dell’ Istruzione, dell’ Università e della Ricerca” (PRIN) is gratefully acknowledged.

REFERENCES

Albunia, A. R., Rizzo, P., and Guerra, G. (2013). Control of guest transport in polymer films by structure and orientation of nanoporous-crystalline phases. *Polymer* 54, 1671–1678. doi: 10.1016/j.polymer.2013.01.027

- Alexandre, M., and Dubois, P. (2000). Polymer layered silicate nanocomposites: preparation, properties and uses of a new class of materials. *Mater. Sci. Eng. R. Rep.* 28, 1–63. doi: 10.1016/S0927-796X(00)00012-7
- Anderson, M. L., Stroud, R. M., and Rolison, D. R. (2002). Enhancing the activity of fuel-cell reactions by designing three-dimensional nanostructured architectures, catalyst-modified carbon-silica composite aerogels. *Nano Lett.* 2, 235–240. doi: 10.1021/nl015707d
- Baker, K. C., Manitiu, M., Bellair, R., Gratopp, C. A., Herkowitz, H. N., and Kannan, R. M. (2011). Supercritical carbon dioxide processed resorbable polymer nanocomposite bone graft substitutes. *Acta Biomater.* 7, 3382–3389. doi: 10.1016/j.actbio.2011.05.014
- Bandi, S., Bell, M., and Schiraldi, D. A. (2005). Temperature-responsive clay aerogel-polymer composites. *Macromolecules* 38, 9216–9220. doi: 10.1021/ma051698+
- Bergaya, F., and Lagaly, G. (2013). *Handbook of Clay Science*. 2nd Edn. Elsevier, Amsterdam.
- Bergaya, F. A. (2008). Layered clay minerals: basic research and innovative composite applications. *Microp. Mesop. Mater.* 107, 141–148. doi: 10.1016/j.micromeso.2007.05.064
- Buonerba, A., Cuomo, C., Ortega Sánchez, S., Canton, P., and Grassi, A. (2012). Gold nanoparticles incarcerated in nanoporous syndiotactic polystyrene matrices as new and efficient catalysts for alcohol oxidations. *Chem. Eur. J.* 18, 709–715. doi: 10.1002/chem.201101034
- Buono, A., Rizzo, P., Immediata, I., and Guerra, G. (2009). Detection and memory of nonracemic molecules by a racemic host polymer film. *J. Am. Chem. Soc.* 129, 10992–10993. doi: 10.1021/ja0732936
- Chen, B., Evans, J. R. G., Greenwell, H. C., Boulet, P., Coveney, P. V., Bowden, A. A., et al. (2008). A critical appraisal of polymer-clay nanocomposites. *Chem. Soc. Rev.* 37, 568–594. doi: 10.1039/b702653f
- Chen, C., Samaniuk, J., Baird, D. G., Devoux, G., Zhang, M., Moore, R. B., et al. (2012). The preparation of nano-clay/polypropylene composite materials with improved properties using supercritical carbon dioxide and a sequential mixing technique. *Polymer* 53, 1373–1382. doi: 10.1016/j.polymer.2012.01.049
- Choi, Y. S., Ham, H. T., and Chung, I. (2004). Effect of monomers on the basal spacing of sodium montmorillonite and the structures of polymer-clay nanocomposites. *J. Chem. Mater.* 16, 2522–2529. doi: 10.1021/cm0348601
- Chou, C. C., and Lin, J. (2005). One-step exfoliation of montmorillonite via phase inversion of amphiphilic copolymer emulsion. *Macromolecules* 38, 230–233. doi: 10.1021/ma047761x
- Cipolletti, V., Galimberti, M., Guerra, G., and Mauro, M. (2013). Organoclays with hexagonal rotator order for the paraffinic chains of the compensating cation. Implications on the structure of clay polymer nanocomposites. *Appl. Clay Sci.* doi: 10.1016/j.clay.2013.11.001
- Cusano, A., Iadicco, A., Pilla, P., Contessa, L., Campopiano, S., Cutolo, A., et al. (2006). Coated long-period fiber gratings as high-sensitivity optochemical sensors. *J. Lightw. Technol.* 24, 1776–1786. doi: 10.1109/JLT.2006.871128
- Daniel, C., Alfano, D., Venditto, V., Cardea, S., Reverchon, E., Larobina, D., et al. (2005). Aerogels with microporous crystalline host phase. *Adv. Mater.* 17, 1515–1518. doi: 10.1002/adma.200401762
- Daniel, C., Giudice, S., and Guerra, G. (2009). Syndiotactic polystyrene aerogels with beta, gamma and epsilon crystalline phases. *Chem. Mater.* 21, 1028–1034. doi: 10.1021/cm802537g
- Daniel, C., Longo, S., Cardea, S., Vitillo, J. G., and Guerra, G. (2012). Monolithic nanoporous-crystalline aerogels based on PPO. *RSC Adv.* 2, 12011–12018. doi: 10.1039/c2ra22325b
- Daniel, C., Longo, S., Ricciardi, R., Reverchon, E., and Guerra, G. (2013a). Monolithic nanoporous crystalline aerogels. *Macromol. Rapid. Commun.* 34, 1194–1207. doi: 10.1002/marc.201300260
- Daniel, C., Zhovner, D., and Guerra, G. (2013b). Thermal stability of nanoporous crystalline and amorphous phases of poly(2, 6-dimethyl-1, 4-phenylene)oxide. *Macromolecules* 46, 449–454. doi: 10.1021/ma302227q
- Daniel, C., Longo, S., Vitillo, J. G., Fasano, G., and Guerra, G. (2011). Nanoporous crystalline phases of poly(2, 6-dimethyl-1, 4-phenylene)oxide. *Chem. Mater.* 23, 3195–3200. doi: 10.1021/cm200546r
- Daniel, C., Sannino, D., and Guerra, G. (2008). Syndiotactic polystyrene aerogels: adsorption in amorphous pores and absorption in crystalline nanocavities. *Chem. Mater.* 20, 577–582. doi: 10.1021/cm702475a

- De Rosa, C., Guerra, G., Petraccone, V., and Pirozzi, B. (1997). Crystal structure of the emptied clathrate form (δ form) of syndiotactic polystyrene. *Macromolecules* 30, 4147–4152. doi: 10.1021/ma970061q
- Erdogan, M., Ozbek, Z., Capan, R., and Yagci, Y. (2012). Characterization of polymeric LB thin films for sensor applications. *J. Appl. Polym. Sci.* 123, 2414–2422. doi: 10.1002/app.34793
- Feng-hua, S., Han-xiong, H., and Yang, Z. (2011). Microstructure and mechanical properties of polypropylene/poly(ethylene-co-octene copolymer)/clay ternary nanocomposites prepared by melt blending using supercritical carbon dioxide as a processing aid. *Compos. Part B* 42, 421–428. doi: 10.1016/j.compositesb.2010.12.005
- Galimberti, M. (ed.). (2011). *Rubber Clay Nanocomposites-Science, Technology and Applications*. New York, NY: Wiley and Sons. doi: 10.1002/9781118092866
- Galimberti, M., Giudice, S., Cipolletti, V., and Guerra, G. (2010). Control of organo-clay structure in hydrocarbon polymers. *Polym. Adv. Tech.* 21, 1–6. doi: 10.1002/pat.1757
- Galimberti, M., Lostritto, A., Spatola, A., and Guerra, G. (2007). Clay delamination in hydrocarbon rubbers. *Chem. Mater.* 19, 2495–2499. doi: 10.1021/cm062782m
- Galimberti, M., Senatore, S., Conzatti, L., Costa, G., Giuliano, G., and Guerra, G. (2009). Formation of clay intercalates with organic bilayers in hydrocarbon polymers. *Polym. Adv. Technol.* 20, 135–142. doi: 10.1002/pat.1287
- Galizia, M., Daniel, C., Fasano, G., Guerra, G., and Mensitieri, G. (2012). Gas sorption and diffusion in amorphous and semicrystalline nanoporous poly(2, 6-dimethyl-1, 4-phenylene)oxide. *Macromolecules* 45, 3604–3615. doi: 10.1021/ma3000626
- Giordano, M., Russo, M., Cusano, A., Mensitieri, G., and Guerra, G. (2005). Syndiotactic polystyrene thin film as sensitive layer for an optoelectronic chemical sensing device. *Sens. Actuators B* 109, 177–184. doi: 10.1016/j.snb.2004.02.053
- Gowd, E. B., Shibayama, N., and Tashiro, K. (2006). Structural changes in thermally induced phase transitions of uniaxially oriented δ_c form of syndiotactic polystyrene investigated by temperature-dependent measurements of X-Ray fiber diagrams and polarized infrared spectra. *Macromolecules* 39, 8412–8418. doi: 10.1021/ma061659d
- Grassi, A., Pellicchia, C., Longo, P., and Zambelli, A. (1987). Selective synthesis of syndiotactic polystyrene. *Gazz. Chim. Ital.* 117, 249–250.
- Horsch, S., Serhatkulu, G., Gulari, E., and Kannan, R. M. (2006). Supercritical CO₂ dispersion of nano-clays and clay/polymer nanocomposites. *Polymer* 47, 7485–7496. doi: 10.1016/j.polymer.2006.08.048
- Ide, Y., and Ogawa, M. (2006). Preparation and some properties of organically modified layered alkali titanates with alkylmethoxysilanes. *J. Colloid. Interface Sci.* 296, 141–149. doi: 10.1016/j.jcis.2005.08.058
- Itoh, T., Ohta, N., Shichi, T., Yui, T., and Takagi, K. (2003). The self-assembling properties of stearate ions in hydrotalcite clay composites. *Langmuir* 19, 9120–9126. doi: 10.1021/la0302448
- Kistler, S. S. (1931). Coherent expanded aerogels and jellies. *Nature* 127, 741. doi: 10.1038/127741a0
- Kojima, Y., Usuki, A., Kawasumi, M., Okada, A., Fukushima, Y., Kurauchi, et al. (1993). Mechanical properties of nylon 6-clay hybrid. *J. Mater. Res.* 8, 1179–1185. doi: 10.1557/JMR.1993.1185
- Kucheyev, S. O., Stadermann, M., Shin, S. J., Satcher, J. H., Gammon, S. A., Letts, S. A., et al. (2012). Super-compressibility of ultralow-density nanoporous silica. *Adv. Mater.* 24, 776–780. doi: 10.1002/adma.201103561
- LeBaron, P. C., Wang, Z., and Pinnavaia, T. J. (1999). Polymer-layered silicate nanocomposites: an overview. *Appl. Clay Sci.* 15, 11–29. doi: 10.1016/S0169-1317(99)00017-4
- Longo, S., Vitillo, J. G., Daniel, C., and Guerra, G. (2013). Monolithic aerogels Based on poly(2, 6-diphenyl-1, 4-phenylene oxide) and syndiotactic polystyrene. *ACS Appl. Mater. Interfaces* 5, 5493–5499. doi: 10.1021/am400592z
- Ma, J., Bilotti, E., Peijs, T., and Darr, J. A. (2007). Preparation of polypropylene/sepiolite nanocomposites using supercritical CO₂ assisted mixing. *Eur. Polym. J.* 43, 4931–4939. doi: 10.1016/j.eurpolymj.2007.09.010
- Mahesh, K. P. O., Sivakumar, M., Yamamoto, Y., Tsujita, Y., Yoshimizu, H., and Okamoto, S. (2005). Structure and properties of the mesophase of syndiotactic polystyrene. *J. Membrane Sci.* 262, 11–19. doi: 10.1016/j.memsci.2005.04.002
- Malik, S., Roizard, D., and Guenet, J. M. (2006). Multiporous material from fibrillar syndiotactic polystyrene intercalates. *Macromolecules* 39, 5957–5959. doi: 10.1021/ma060770g
- Manfredi, C., Del Nobile, M. A., Mensitieri, G., Guerra, G., and Rapacciuolo, M. (1997). Vapor sorption in emptied clathrate samples of syndiotactic polystyrene. *J. Polym. Sci. Polym. Phys. Ed.* 35, 133–140. doi: 10.1002/(SICI)1099-0488(19970115)35:1<133::AID-POLB11>3.0.CO;2-E
- Manias, E., Touny, A., Wu, L., Strawhecker, K., Lu, B., and Chung, T. C. (2001). Polypropylene/Montmorillonite nanocomposites. Review of the synthetic routes and materials properties. *Chem. Mater.* 13, 3516–3523. doi: 10.1021/cm0110627
- Manitiu, M., Bellair, R. J., Horsch, S., Gulari, E., and Kannan, R. M. (2008). Supercritical carbon dioxide-processed dispersed polystyrene-clay nanocomposites. *Macromolecules* 41, 8038–8046. doi: 10.1021/ma801339g
- Mauro, M., Maggio, M., Cipolletti, V., Galimberti, M., Longo, P., and Guerra, G. (2013). Graphite oxide intercalation compounds with rotator hexagonal order in the intercalated layers. *Carbon* 61, 395–403. doi: 10.1016/j.carbon.2013.05.023
- Mensitieri, G., Venditto, V., and Guerra, G. (2003). Polymeric sensing films absorbing organic guests into a nanoporous host crystalline phase. *Sens. Actuators B* 92, 255–261. doi: 10.1016/S0925-4005(03)00273-9
- Milano, G., Venditto, V., Guerra, G., Cavallo, L., Ciambelli, P., and Sannino, D. (2001). Shape and volume of cavities in thermoplastic molecular sieves based on syndiotactic polystyrene. *Chem. Mater.* 13, 1506–1511. doi: 10.1021/cm001089a
- Musto, P., Mensitieri, G., Cotugno, S., Guerra, G., and Venditto, V. (2002). Probing by time-resolved FTIR spectroscopy mass transport, molecular interactions, and conformational ordering in the system chloroform-syndiotactic polystyrene. *Macromolecules* 35, 2296–2304. doi: 10.1021/ma011684d
- Nguyen, Q. T., and Baird, D. G. (2007). An improved technique for exfoliating and dispersing nanoclay particles into polymer matrices using supercritical carbon dioxide. *Polymer* 48, 6923–6933. doi: 10.1016/j.polymer.2007.09.015
- Osman, M. A., Ernst, M., Meier, B. H., and Suter, U. W. (2002). Structure and molecular dynamics of alkane monolayers self-assembled on mica platelets. *J. Phys. Chem. B* 106, 653–662. doi: 10.1021/jp0132376
- Park, Y., Ayoko, G. A., and Frost, R. L. (2011). Characterisation of organoclays and adsorption of p-nitrophenol: environmental application. *J. Colloid Interface Sci.* 360, 440–456. doi: 10.1016/j.jcis.2011.04.085
- Paul, D. R., and Robeson, L. M. (2008). Polymer nanotechnology: nanocomposites. *Polymer* 49, 3187–3204. doi: 10.1016/j.polymer.2008.04.017
- Petraccone, V., Ruiz de Ballesteros, O., Tarallo, O., Rizzo, P., and Guerra, G. (2008). Nanoporous polymer crystals with cavities and channels. *Chem. Mater.* 20, 3663–3668. doi: 10.1021/cm800462h
- Pilla, P., Cusano, A., Cutolo, A., Giordano, M., Mensitieri, G., Rizzo, P., et al. (2009). Molecular sensing by nanoporous crystalline polymers. *Sensors* 9, 9816–9857. doi: 10.3390/s91209816
- Pojanavaraphan, T., Liu, L., Ceylan, D., Okay, O., Magaraphan, R., and Schiraldi, D. A. (2011). Solution cross-linked natural rubber (NR)/clay aerogel composites. *Macromolecules* 44, 923–931. doi: 10.1021/ma102443k
- Pojanavaraphan, T., Schiraldi, D. A., and Magaraphan, R. (2010). Mechanical, rheological, and swelling behavior of natural rubber/montmorillonite aerogels prepared by freeze-drying. *Appl. Clay Sci.* 50, 271–279. doi: 10.1016/j.clay.2010.08.020
- Powder diffraction database 70-2151 International Centre for Diffraction Data. (1999). *PCPDF win. Version 2.02*.
- Ray, S. S., and Okamoto, M. (2003). Polymer/layered silicate nanocomposites: a review from preparation to processing. *Prog. Polym. Sci.* 28, 1539–1641. doi: 10.1016/j.progpolymsci.2003.08.002
- Rizzo, P., Daniel, C., De Girolamo Del Mauro, A., and Guerra, G. (2007). New host polymeric framework and related polar guest cocrystals. *Chem. Mater.* 19, 3864–3866. doi: 10.1021/cm071099c
- Robello, D. R., Yamaguchi, N., Blanton, T., and Barnes, C. (2004). Spontaneous formation of an exfoliated polystyrene-clay nanocomposite using a star-shaped polymer. *J. Am. Chem. Soc.* 126, 8118–8119. doi: 10.1021/ja048211h
- Samaniuk, J., Litchfield, D., and Baird, D. (2009). Improving the exfoliation of layered silicate in a poly(ethylene terephthalate) matrix using supercritical carbon dioxide. *Polym. Eng. Sci.* 49, 2329–2341. doi: 10.1002/pen.21482
- Schaefer, D. W., and Keefer, K. D. (1986). Restructuring of colloidal silica aggregates. *Phys. Rev. Lett.* 56, 2199. doi: 10.1103/PhysRevLett.56.2199

- Tarallo, O., Petraccone, V., Daniel, C., Fasano, G., Rizzo, P., and Guerra, G. (2012). A chiral co-crystalline form of poly(2, 6-dimethyl-1, 4-phenylene)oxide (PPO). *J. Mater. Chem.* 22, 11672–11680. doi: 10.1039/c2jm30907f
- Thompson, M. R., Balogh, M. P., Speer, R. L., Fasulo, P. D., and Rodgers, W. R. (2009). In situ X-ray diffraction studies of alkyl quaternary ammonium montmorillonite in a CO₂ environment. *J. Chem. Phys.* 130, 044705. doi: 10.1063/1.3065980
- Treece, M. A., and Oberhauser, J. P. (2007). Processing of polypropylene-clay nanocomposites: single screw extrusion with in-line supercritical carbon. *J. Appl. Polym. Sci.* 103, 884–892. doi: 10.1002/app.25226
- Vaia, R. A., Ishii, H., and Giannelis, E. P. (1993). Synthesis and properties of two dimensional nanostructures by direct intercalation of polymer melts in layered silicates. *Chem. Mater.* 5, 1694–1696. doi: 10.1021/cm00036a004
- Venditto, V., De Girolamo Del Mauro, A., Mensitieri, G., Milano, G., Musto, P., Rizzo, P., et al. (2006). Anisotropic guest diffusion in the δ crystalline host phase of syndiotactic polystyrene: transport kinetics in films with three different uniplanar orientations of the host phase. *Chem. Mater.* 18, 2205–2210. doi: 10.1021/cm051657s
- Wang, X., and Jana, S. C. (2013). Syndiotactic polystyrene aerogels containing multi-walled carbon nanotubes. *Polymer* 54, 750–759. doi: 10.1016/j.polymer.2012.12.025
- Wang, Y., Alhassan, S. M., Yang, V. H., and Schiraldi, D. A. (2013). Polyether-block-amide copolymer/clay films prepared via a freeze-drying method. *Compos. Part B* 45, 625–630. doi: 10.1016/j.compositesb.2012.05.017
- Wei, T. Y., Chen, C. H., Chang, K. H., Lu, S. Y., and Hu, C. C. (2010). A Cost-effective supercapacitor material of ultrahigh specific capacitances: spinel nickel cobaltite aerogels from an epoxide-driven sol-gel process. *Adv. Mater.* 22, 347–351. doi: 10.1002/adma.200902175

Conflict of Interest Statement: The authors declare that the research was conducted in the absence of any commercial or financial relationships that could be construed as a potential conflict of interest.

Received: 29 August 2013; paper pending published: 20 September 2013; accepted: 14 October 2013; published online: 13 November 2013.

Citation: Longo S, Mauro M, Daniel C, Galimberti M and Guerra G (2013) Clay exfoliation and polymer/clay aerogels by supercritical carbon dioxide. *Front. Chem.* 1:28. doi: 10.3389/fchem.2013.00028

This article was submitted to *Polymer Chemistry*, a section of the journal *Frontiers in Chemistry*.

Copyright © 2013 Longo, Mauro, Daniel, Galimberti and Guerra. This is an open-access article distributed under the terms of the Creative Commons Attribution License (CC BY). The use, distribution or reproduction in other forums is permitted, provided the original author(s) or licensor are credited and that the original publication in this journal is cited, in accordance with accepted academic practice. No use, distribution or reproduction is permitted which does not comply with these terms.